

RESEARCH ARTICLE

Mathematical modelling of fiber optic cable with an electro-optical cladding by incommensurate fractional-order differential equations

Büşra Ersoy^a, Bahatdin Daşbaşı^b, Ekin Aslan^{a*}

^aDepartment of Electrical and Electronics Engineering, Kayseri University, Turkey

^bDepartment of Engineering Basic Sciences, Kayseri University, Turkey
bsersoy38@gmail.com, bdasbasi@kayseri.edu.tr, ekinaslan@kayseri.edu.tr

ARTICLE INFO

Article History:

Received 3 February 2023

Accepted 11 September 2023

Available Online 12 December 2023

Keywords:

Electro-optical fiber

Fractional-order differential equations (FODEs)

Mathematical model

Stability analysis

AMS Classification 2010:

26A33; 78A05

ABSTRACT

In this study, the mathematical model through incommensurate fractional-order differential equations in Caputo meaning are presented for time-dependent variables given as the numerical aperture, critical angle, and acceptance angle characteristics of a fiber optic cable with electro-optical cladding. The qualitative analysis including the existence and stability of the equilibrium points of the proposed model has been made according to the used parameters, and then, the results obtained from this analysis are supported through numerical simulations by giving the possible values that can be obtained from experimental studies to these parameters in the model. In this way, a stable equilibrium point of the system for the core refractive index, cladding refractive index and electrical voltage is obtained according to the threshold parameter. Thus, the general formulas for the critical angle, acceptance angle and numerical aperture have been obtained when this fixed point is stable.



1. Introduction

Optical fibers are referred to as the waveguide used for light transmission [1]. The light signal includes modulated information and is carried over the glass surface due to the structure of the fiber [2]. Modern optical fibers consist of two coaxial glass cylinders, consisting of the outer layer called cladding and the inner layer called the essence with a larger refractive index [3]. The structure of the optical fiber is depicted in Figure 1.

The phenomenon of total internal reflection is a necessary condition for the transmission of light within the waveguide. Otherwise, efficient transmission does not occur, that is, the light passes to the external environment. Furthermore, gauges such as optical fibers' refractive index profiles, structures, the number of modes they support, signal processing capabilities, distribution, and

polarization can also classify them. The phenomenon of total reflection can be explained by Snell's law, which represents the phenomenon of beam optics at the interface separating two different media [1] and is expressed as $n_1 \sin \theta_1 = n_2 \sin \theta_2$.

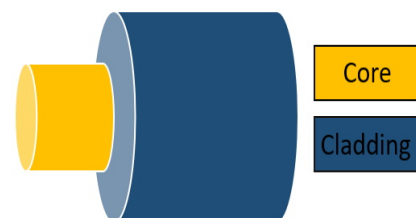


Figure 1. The basic structure of the optical fiber.

When a light beam encounters an interface separating two different environments, some of the

*Corresponding Author

light is reflected in the first environment and the rest passes to the second medium. This is because the speed of light is different in the two environments. Figure 2 shows the behavior of the light beam when it encounters the interface. Here, the relationship between refractive indices is $n_1 > n_2$ [4–6].

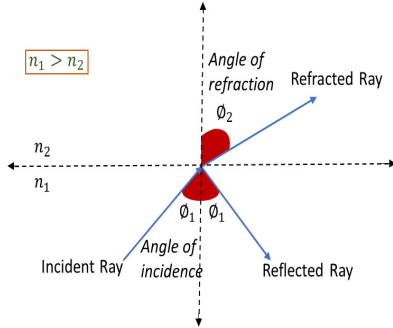


Figure 2. The behavior of the light beam encountering an interface.

Assuming that the angle of refraction is 90° , the expression $\theta_c = \sin^{-1}\left(\frac{n_2}{n_1}\right)$ is reached and θ_c is known as the critical angle [7,8]. If the angle of θ_1 made by the incoming beam with the normal of the interface is greater than the critical angle, the total internal reflection criterion is met and the light is reflected back to the initial environment at exactly the same angle [7–9]. The refractive indices, critical angle, acceptance angle, and acceptance cone of the core, cladding, and external environment on the fiber optic cable operating on the total reflection principle are stated in Figure 3.

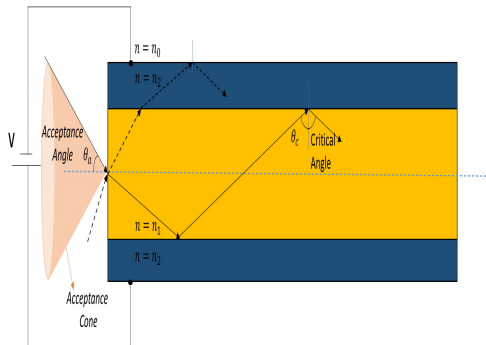


Figure 3. The refractive indices, critical angle, acceptance angle and acceptance cone of the core, cladding and external environment on the fiber optic cable.

One of the parameters that determine the performance of optical fibers is the numerical aperture (NA), whose formula is $NA = n_0 \sin \theta_a = (n_1^2 - n_2^2)^{1/2}$ [7]. Here θ_a is the angle of acceptance [8]. NA is the capacity to capture light rays of different angles entering the fiber optic

cable. The larger the NA magnitude, the more light beams travel through the fiber. Fibers have a certain angle of acceptance, and this angle varies depending on the refractive index of the core, cladding, and medium from which the light comes. Fiber optic cable can only transmit incoming light rays within the limits of the acceptance cone angle, and another performance criterion, the acceptance angle is half the acceptance cone angle. NA grows as the difference between the core and cladding indices of fiber optic cable grows [7,8,10].

The development of optical fibers is possible through close cooperation between both waveguide and materials engineering [11,12]. Functionality can be added to fiber optic cables with the adjustable behavior of materials. A variation in refractive indices of electro-optical (EO) materials, whose optical effects can be adjusted, can be observed with an externally applied electric field. In this context, there are many studies on EO waveguide modulators and optical fibers in the literature. The first study on EO polymer optical fiber (POF) has been proposed by Kuzyk et al [13–19]. Here, high electrical strength has been obtained with an optical fiber consisting of cladding with two parallel indium electrodes, doped EO cores and poly (methyl methacrylate) (PMMA) cladding.

In another study, a few important factors related to the creation and sustainability of EO effect in POF have been examined experimentally and several EO POF designs have been presented. One of the designs is a dual-core-planar cladding while the other designs are a dual-core design with one EO core and an H-shaped cladding in section. In the study, the EO effect of the structure has been measured and the change of this effect in different conditions has been examined. In the same article, it is emphasized that many device applications are based on the EO effect and it is also stated that they plan to improve liquid crystal doped POFs [13]. In this study, the refractive index change caused by the EO effect of the material with the external electric field applied to the cladding from the outside is defined in the proposed mathematical model.

A mathematical model is an abstract model made using mathematical symbols and objects to explain the behavior of a real-life situation. This type of modeling can help make better decisions and examine functional relationships by making predictions about a particular process [20]. It can be submitted in many different versions, such as mathematical models, statistical models, and differential equations. Differential equation models

are used in many fields of science to determine the dynamic perspectives of systems. Fractional calculus has been an ancient but increasingly important subject of mathematics since the 17th century. Fractional integral and differential operators can be thought of as generalized forms of integral and derivative operators with non-integer order [21]. The memory notion for fractional calculus is significant. In memory systems, it has to remember previous values of the input to indicate the current value of the output. Considering the modeling of various memory phenomena, it is generally stated that a memory process is composed two phases, a short-term situation with permanent retention and a situation through fractional derivative [22]. Recently, an increasing number of studies and applications of fractional order systems have been presented in many fields of science and engineering [23–26].

The innovation in this study is to propose the fractional-order differential equation model for the fiber optic consisting of EO cladding, such that the dependent variables are the external electric field applied externally to the cladding and the changes in refractive index caused by the EO effect of the material.

Therefore, the structure of this article is formatted in the following order. In Section 2, we submit some mathematical definitions and notations regarding fractional-order differential equations adopted in the article. In Section 3, the mathematical model for an electro-optic cladding fiber optic cable is introduced and then it has been carried out the qualitative analysis of this model. Also, the formulas for the structural parameters of optical fiber waveguides have been updated, when the system is in equilibrium. The proposed method is numerically examined by a sample in Section 4. Finally, the results and discussion are drawn in Section 5.

2. Preliminaries of fractional-order derivative

This section reviews the fundamental definitions, theorems, concepts, and results that we will use throughout the remainder of this paper.

Definition 1. (Riemann–Liouville fractional integral) Let $t_0 \in \mathbb{R}_+ = [0, \infty)$ be the initial time. Let $L_1^{loc}(J, \mathbb{R}^n)$ be the linear space of all locally Lebesgue integrable functions $m : J \rightarrow \mathbb{R}^m$, $J \subset \mathbb{R}$. Let $\|\cdot\|$ be a norm in \mathbb{R}^n . Riemann–Liouville fractional integral of order $\alpha \in (0, 1)$

$${}_t I_t^\alpha m(t) = \frac{1}{\Gamma(\alpha)} \int_{t_0}^t \frac{m(s)}{(t-s)^{1-\alpha}} ds, \quad t \geq t_0, \quad (1)$$

where $m \in L_1^{loc}([t_0, \infty), \mathbb{R})$ and $\Gamma(\cdot)$ is the Gamma function [27].

Definition 2. (Caputo fractional derivative) The Caputo fractional-order differential operator of the function X can be stated as

$$\begin{cases} {}_t^C D_t^\alpha X(t) = \frac{1}{\Gamma(m-\alpha)} \int_a^t \frac{X^{(m)}(\tau)}{(t-\tau)^{\alpha-m+1}} d\tau \text{ for } m-1 < \alpha < m, \\ X^{(m)}(\tau) \text{ for } \alpha = m, \end{cases} \quad (2)$$

where $t_0 \leq t$, $m \in \mathbb{Z}^+$ [27].

Lemma 1. (Generalized mean value theorem) Assume that $X(t) \in C([a, b])$ and ${}_t^C D_t^\alpha X(t) \in C([a, b])$, such that $0 < \alpha \leq 1$, then:

$$X(t) = X(a) + \frac{1}{\Gamma(\alpha)} {}_t^C D_t^\alpha X(\xi) (t-a)^\alpha, \quad (3)$$

with $a \leq \xi \leq t$, for all $t \in (a, b]$ [28, 29].

Definition 3. (Incommensurate fractional order system) The multi-order fractional differential equation system reads as

$${}_t^C D_t^\alpha X(t) = F(t, X), \quad X(0) = X_0 \quad (4)$$

where $X(t) = [x_1(t), x_2(t), \dots, x_n(t)]^T \in \mathbb{R}^n$, $F = [f_1, f_2, \dots, f_n]^T \in \mathbb{R}^n$, $f_i : [0, +\infty) \times \mathbb{R}^n \rightarrow \mathbb{R}$, $i = 1, 2, \dots, n$. $\alpha = [\alpha_1, \alpha_2, \dots, \alpha_n]$ is the multi-order of system (4), if all α_i are equal to a constant, then (4) is the generally considered model. ${}_t^C D_t^\alpha = [{}_t^C D_t^{\alpha_1}, {}_t^C D_t^{\alpha_2}, \dots, {}_t^C D_t^{\alpha_n}]^T$, ${}_t^C D_t^{\alpha_i}$ denotes α_i th-order fractional derivative in the Caputo sense. ${}_t^C D_t^\alpha X(t)$ refers to the “direct product” of linear operator ${}_t^C D_t^\alpha$ and vector $X(t)$, i.e. ${}_t^C D_t^\alpha X(t) = [{}_t^C D_t^{\alpha_1} x_1(t), {}_t^C D_t^{\alpha_2} x_2(t), \dots, {}_t^C D_t^{\alpha_n} x_n(t)]^T$ [30]. The multiple order can be any real vector, even a complex one. In this study, it is only accepted the real case of order.

If $\alpha = \alpha_1 = \alpha_2 = \dots = \alpha_n$, then the system is called a commensurate order system, otherwise system denotes an incommensurate order system (IFOS), which is more general than the other [31].

Definition 4. The equilibrium points of system (4) are calculated by solving the following equation $F(X) = 0$ and we have been supposed that $X^* = (x_1^*, x_2^*, \dots, x_n^*)$ is an equilibrium point of system (4).

Lemma 2. Eigenvalues λ_i for $i = 1, 2, \dots$, $\rho(\alpha_1 + \alpha_2 + \dots + \alpha_n)$ of system (4)

are calculated by the characteristic polynomial obtained from

$\det(\text{diag}(\lambda^{\rho\alpha_1}, \lambda^{\rho\alpha_2}, \dots, \lambda^{\rho\alpha_n}) - J(X^*)) = 0$ such that ρ is the least common multiple of the denominators of rational numbers $\alpha_1, \alpha_2, \dots, \alpha_n$ and $J(X^*) = \frac{\partial F}{\partial X}|_{X=X^*}$. If all eigenvalues λ_i satisfy $|\arg(\lambda_i)| > \frac{\pi}{2\rho}$, then X^* is locally asymptotically stable (LAS) for system (4) [32, 33].

3. The mathematical model for an electro-optic cladding fiber optic cable

This section of the paper purposes to suggest a model based on the memorability nature of the Caputo fractional-order derivative. Let the t (≥ 0) value represent the time parameter. It is denoted the voltage of the electric field by v , the refractive index of the core of the fiber optic cable by n_1 , and the cladding refractive index by n_2 . Also, it is $v = v(t)$, $n_1 = n_1(t)$, $n_2 = n_2(t)$ such that $v, n_1, n_2 > 0$. Our recommended model described the changes in the refractive indexes of fiber optic cable with electro-optic cladding is expressed by the following IFOS

$$\begin{aligned} {}_0^C D_t^{\alpha_1} v(t) &= \Lambda - \beta v \\ {}_0^C D_t^{\alpha_2} n_1(t) &= r_1 n_1 \left(1 - \frac{n_1}{C}\right) \\ {}_0^C D_t^{\alpha_3} n_2(t) &= r_2 n_2 \left(1 - \frac{n_2}{n_1}\right) - \delta v + n_0 \end{aligned} \quad (5)$$

with positive initial conditions $v(0) = v_0$, $n_1(0) = n_{10}$, $n_2(0) = n_{20}$. In addition that, the derivative orders are α_i for $i = 1, 2, 3$ such that $0 < \alpha_i \leq 1$ and the parameters have the properties given as

$$\Lambda, \beta, r_1, C, r_2, \delta, n_0 > 0. \quad (6)$$

The model has the following assumptions. The voltage is supplied by the fixed amount of Λ and it is decreasing by a ratio β . It is also assumed that the inequality

$$\frac{n_0}{\delta} \geq v \quad (7)$$

exists for v . For the refractive index of the core of the fiber optic cable (n_1) and the refractive index of the cladding (n_2), their sizes vary according to the logistic rules. The rate of increase of n_1 is r_1 and its maximum magnitude (the mathematically well-known the carrying capacity term) is C . Also, it is always $n_1 > n_2$. Therefore, the maximum magnitude of the refractive index of the cladding is up to or smaller than the refractive index of the core of the fiber optic cable. The

growth rate of the refractive index of the cladding is r_2 . Also, n_2 decreases by its δ ratio as it is affected by the voltage of the electric field. Since n_0 , which is the refractive index of the medium outside the fiber optic cable, is smaller than n_2 , n_0 has been added to the cladding refractive index.

3.1. The existence and uniqueness of the solution of system (5)

In this section, the existence and uniqueness of the solutions for FOS in Eqs (5) is examined.

Lemma 3. *With each non-negative initial conditions, there exists a unique solution of fractional-order system in Eqs (3). For every non-negative initial condition, there is a unique solution of fractional-order system in Eqs (5).*

Proof. Existence and uniqueness of system (3) will be indicated in the region $\Omega \times (0; T]$ where $\Omega = \{(v, n_1, n_2) \in \mathbb{R}_+^3 : \max(|v|, |n_1|, |n_2|) \leq \zeta\}$. Here, it is followed the approach used in [32]. We express $X = (v, n_1, n_2)$ and $\bar{X} = (\bar{v}, \bar{n}_1, \bar{n}_2)$. Consider a mapping

$$G(X) = (G_1(X), G_2(X), G_3(X))$$

and

$$\begin{aligned} G_1(X) &= \Lambda - \beta v, \\ G_2(X) &= r_1 n_1 \left(1 - \frac{n_1}{C}\right), \\ G_3(X) &= r_2 n_2 \left(1 - \frac{n_2}{n_1}\right) - \delta v + n_0. \end{aligned} \quad (8)$$

For any X, \bar{X} , it follows from (8) that $\|G(X) - G(\bar{X})\| = |\Lambda - \beta v - \Lambda + \beta \bar{v}| + \left|r_1 n_1 \left(1 - \frac{n_1}{C}\right) - r_1 \bar{n}_1 \left(1 - \frac{\bar{n}_1}{C}\right)\right| + \left|r_2 n_2 \left(1 - \frac{n_2}{n_1}\right) - \delta v + n_0 - r_2 \bar{n}_2 \left(1 - \frac{\bar{n}_2}{\bar{n}_1}\right) + \delta \bar{v} - n_0\right| = \beta |v - \bar{v}| + \left|r_1 (n_1 - \bar{n}_1) - \frac{r_1}{C} (n_1 - \bar{n}_1)(n_1 + \bar{n}_1)\right| + \left|r_2 (n_2 - \bar{n}_2) - r_2 \left(n_2 \frac{n_2}{n_1} - \bar{n}_2 \frac{\bar{n}_2}{\bar{n}_1}\right) - \delta (v - \bar{v})\right|,$

$$\|G(X) - G(\bar{X})\| \leq \beta |v - \bar{v}| + r_1 |(n_1 - \bar{n}_1)| + \frac{r_1}{C} |(n_1 - \bar{n}_1)| |(n_1 + \bar{n}_1)| + |r_2 (n_2 - \bar{n}_2)| + r_2 \left| \left(n_2 \frac{n_1}{n_2} - \bar{n}_2 \frac{\bar{n}_1}{\bar{n}_2}\right) \right| + \delta |(v - \bar{v})|,$$

$$\|G(X) - G(\bar{X})\| \leq (\beta + \delta) |v - \bar{v}| + \left(r_1 + \frac{r_1}{C} |(n_1 + \bar{n}_1)|\right) |n_1 - \bar{n}_1| + r_2 |n_2 - \bar{n}_2| + r_2 \left| \left(\frac{n_2^2}{n_1} - \frac{\bar{n}_2^2}{\bar{n}_1}\right) \right|.$$

We said that the logistic growth rule is valid for n_1 . If the non-negative initial condition ($n_1(0)$) is less than the carrying capacity, it will approach its capacity (C) by increasing, if not, it will approach its capacity by decreasing. For example, let $\max\{n_1, \bar{n}_1\} = n_1$. In this case we have $\left|\frac{n_2^2}{n_1} - \frac{\bar{n}_2^2}{\bar{n}_1}\right| \leq \left|\frac{n_2^2 - \bar{n}_2^2}{n_1}\right| \leq \frac{|n_2 - \bar{n}_2| |n_2 + \bar{n}_2|}{\underbrace{n_1(0)}_{\text{or } C}}$. Therefore, it is

fore, it is

$$\begin{aligned} \|G(X) - G(\bar{X})\| &\leq \varphi_1 |v - \bar{v}| + \varphi_2 |n_1 - \bar{n}_1| \\ &\quad + \varphi_3 |n_2 - \bar{n}_2|, \end{aligned} \tag{9}$$

where

$$\begin{aligned} \varphi_1 &= (\beta + \delta) \\ \varphi_2 &= (r_1 + 2\zeta \frac{r_1}{C}) \\ \varphi_3 &= (r_2 + r_2 \frac{2\zeta}{n_1(0)}) \end{aligned} \tag{10}$$

Therefore, it is obtained $\|G(X) - G(\bar{X})\| \leq L \|X - \bar{X}\|$ where $L = \max(\varphi_1, \varphi_2, \varphi_3)$. $G(X)$ satisfies the Lipschitz condition. In this sense, it is indicated the existence and uniqueness of the solutions of Eqs (5) \square

3.2. Boundedness and non-negativity of the solutions of system(5)

Solutions of Eqs. (5) are non-negative and bounded since they have densities of interacting variables. This case is examined here.

Lemma 4. *The solutions of (3) which start in \mathbb{R}_+^3 are uniformly bounded and non-negative.*

Proof. It is adopted the manner of approaching which is used in [34]. Therefore, we have follows ${}^C D_t^\alpha v(t) = \Lambda - \beta v \Rightarrow v(t) = v(0) E_\alpha(-\beta(t)^\alpha) + \Lambda(t)^\alpha E_{\alpha, \alpha+1}(-\beta(t)^\alpha)$,

$$\begin{aligned} {}^C D_t^\alpha n_1 &\leq r_1 n_1 (1 - \frac{n_1}{C}) \text{ and} \\ {}^C D_t^\alpha n_1 + r_1 n_1 &\leq 2r_1 n_1 - \frac{r_1}{C} n_1^2 = \\ &- \frac{r_1}{C} \left(\overbrace{n_1^2 - 2n_1 C + C^2}^{(n_1 - C)^2} - C^2 \right) \leq r_1 C \Rightarrow n_1(t) \leq \\ n_1(0) E_\alpha(-r_1(t)^\alpha) &+ r_1 C(t)^\alpha E_{\alpha, \alpha+1}(-r_1(t)^\alpha) \end{aligned}$$

$$\lim_{t \rightarrow \infty} n_1(t) \leq C \tag{11}$$

and ${}^C D_t^\alpha n_2 = r_2 n_2 (1 - \frac{n_2}{n_1}) - \delta v + n_0$ and

$$\begin{aligned} {}^C D_t^\alpha n_2 + r_2 n_2 &\leq -\frac{r_2}{n_1} \left(n_2^2 - 2n_2 n_1 + n_1^2 - n_1^2 - \frac{n_0}{r_2} \right) \\ &= \left(-\frac{r_2}{n_1} (n_2 - n_1)^2 + r_2 \left(n_1 + \frac{n_0}{r_2} \right) \right) \leq \\ r_2 \left(C + \frac{n_0}{r_2} \right) &\Rightarrow n_2(t) \leq n_2(0) E_\alpha(-r_2(t)^\alpha) + \\ r_2 \left(C + \frac{n_0}{r_2} \right) (t)^\alpha E_{\alpha, \alpha+1} &(-r_2(t)^\alpha) \end{aligned}$$

$$\lim_{t \rightarrow \infty} n_2(t) \leq \left(C + \frac{n_0}{r_2} \right). \tag{12}$$

Hence, the solutions of FOS starting in \mathbb{R}_+^3 are uniformly bounded in the region Ω .

From the system (5), we have

$$\begin{aligned} {}^C D_t^{\alpha_1} v(t) \Big|_{v=0} &= \Lambda \geq 0 \\ {}^C D_t^{\alpha_2} n_1(t) \Big|_{n_1=0} &= 0 \\ {}^C D_t^{\alpha_3} n_2(t) \Big|_{n_2=0} &= n_0 - \delta v \geq 0 \text{ (Due to (7))} \end{aligned} \tag{13}$$

for all $t \in [0, T]$. With respect to Lemma 1, we can accomplish that the solution $X(t) = (v(t), n_1(t), n_2(t))^T$ of system (5) belongs to \mathbb{R}_+^3 , and this completes the proof. \square

Definition 5. (Threshold Parameter) *To examine the local stability of equilibrium point of Eqs (5), threshold parameter called basic reproduction number has been introduced given as*

$$\mathcal{R}_0 = \frac{(\delta \frac{\Lambda}{\beta} - n_0)}{C r_2}. \tag{14}$$

The stability for equilibrium values of the electric field voltage, the core refractive index of fiber optic cable, and the cladding refractive index of fiber optic cable is defined according to the threshold parameter.

Lemma 5. *Considering equilibrium points of the proposed model in (5) with reference to threshold parameter defined in (14), it is satisfied the followings:*

- i. If $\mathcal{R}_0 \leq 1$, then there is always $E_1 \left(\frac{\Lambda}{\beta}, C, C^{\frac{1+\sqrt{(1-\mathcal{R}_0)}}{2}} \right)$,
- ii. If $0 < \mathcal{R}_0 \leq 1$, then there are both $E_1 \left(\frac{\Lambda}{\beta}, C, C^{\frac{1+\sqrt{(1-\mathcal{R}_0)}}{2}} \right)$ and $E_2 \left(\frac{\Lambda}{\beta}, C, C^{\frac{1-\sqrt{(1-\mathcal{R}_0)}}{2}} \right)$.

Proof. We have assumed that $E(\bar{v}, \bar{n}_1, \bar{n}_2)$ represent the equilibrium point of the system (5), such that

$$\bar{v}, \bar{n}_1, \bar{n}_2 > 0. \tag{15}$$

The steadiness points of system (5) are achieved by deciphering the following system of equations: $Dv^{\alpha_1} = Dn_1^{\alpha_2} = Dn_2^{\alpha_3} = 0$. Therefore, we have

$$\begin{aligned} \Lambda - \beta v &= 0 \\ r_1 n_1 \left(1 - \frac{n_1}{C} \right) &= 0 \\ r_2 n_2 \left(1 - \frac{n_2}{n_1} \right) - \delta v + n_0 &= 0 \end{aligned} \tag{16}$$

From the first two equations of (16), $\bar{n}_1 = C$ and $\bar{v} = \frac{\Lambda}{\beta}$ are obtained. By substituting these values in the last equation, it is obtained the 2nd degree polynomial given as

$$\bar{n}_2^2 - C \bar{n}_2 + \frac{C}{r_2} \left(\delta \frac{\Lambda}{\beta} - n_0 \right) = 0 \tag{17}$$

for the equilibrium value showing the refractive index of the cladding. The discriminant of this equation is $\Delta = C^2(1 - \mathcal{R}_0)$ according to (14). If $\mathcal{R}_0 > 1$, a suitable \bar{n}_2 value cannot be found due to $\Delta < 0$.

- (i) Let $\mathcal{R}_0 \leq 1$. In this case, $(\bar{n}_2)_{1,2} = C^{\frac{1 \pm \sqrt{(1-\mathcal{R}_0)}}{2}}$ for roots of Eq.(17) are obtained. Since it is obvious $(\bar{n}_2)_1 > 0$, the equilibrium point $E_1\left(\frac{A}{\beta}, C, C^{\frac{1+\sqrt{(1-\mathcal{R}_0)}}{2}}\right)$ is reached.
- (ii) Also, the equilibrium point $E_2\left(\frac{A}{\beta}, C, C^{\frac{1-\sqrt{(1-\mathcal{R}_0)}}{2}}\right)$ occurs too, when $\mathcal{R}_0 > 0$.

□

Lemma 6. *The LAS conditions of equilibrium points for the system (5) are as follows.*

- (i) Let $\mathcal{R}_0 < 1$. In this case, $E_1\left(\frac{A}{\beta}, C, C^{\frac{1+\sqrt{(1-\mathcal{R}_0)}}{2}}\right)$ is LAS.
- (ii) The equilibrium point $E_2\left(\frac{A}{\beta}, C, C^{\frac{1-\sqrt{(1-\mathcal{R}_0)}}{2}}\right)$ existing for $0 < \mathcal{R}_0 \leq 1$ is always unstable.

Proof. Let $\mathcal{R}_0 \leq 1$. The Jacobian matrix of the system (5) at $E(\bar{v}, \bar{n}_1, \bar{n}_2)$ for E_1 and/or E_2 is given by

$$J(E(\bar{v}, \bar{n}_1, \bar{n}_2)) = \begin{pmatrix} -\beta & 0 & 0 \\ 0 & r_1 - \frac{2r_1\bar{n}_1}{C} & 0 \\ -\delta & \frac{r_2\bar{n}_2^2}{\bar{n}_1^2} & r_2 - \frac{2r_2\bar{n}_2}{\bar{n}_1} \end{pmatrix} \quad (18)$$

From the equation

$\det(\text{diagonal}(\lambda^{\rho\alpha_1}, \lambda^{\rho\alpha_2}, \lambda^{\rho\alpha_3}) - J(E(\bar{v}, \bar{n}_1, \bar{n}_2))) = 0$, the characteristic equation is

$$(\lambda^{\rho\alpha_1} + \beta)(\lambda^{\rho\alpha_2} - (r_1 - \frac{2r_1\bar{n}_1}{C}))(\lambda^{\rho\alpha_3} - (r_2 - \frac{2r_2\bar{n}_2}{\bar{n}_1})) = 0 \quad (19)$$

where ρ is the least common multiple of the denominators of the derivative orders $\alpha_1, \alpha_2, \alpha_3$ in the system (5). Considering Lemma 2, the LAS condition of $E(\bar{v}, \bar{n}_1, \bar{n}_2)$ is that the λ eigenvalues to be obtained from (19) satisfy the inequalities $\arg(\lambda) > \frac{\pi}{2\rho}$. Also, if λ is real number ($\in \mathbb{R}$), it must be $\lambda < 0$ to satisfy the stability conditions of the equilibrium point. Therefore, it is

$$\lambda^{\rho\alpha_1} = -\beta \quad (20)$$

$$\lambda^{\rho\alpha_2} = r_1 - \frac{2r_1\bar{n}_1}{C} \quad (21)$$

$$\lambda^{\rho\alpha_3} = r_2 - \frac{2r_2\bar{n}_2}{\bar{n}_1} \quad (22)$$

where $\lambda^{\rho\alpha_1}, \lambda^{\rho\alpha_2}, \lambda^{\rho\alpha_3} \in \mathbb{R}$ and $\lambda^{\rho\alpha_1} \in \mathbb{R}^-$ due to inequalities in (6) and (15). Let us consider (20). Therefore, the equations

$$\lambda_j = \beta^{\frac{1}{\rho\alpha_1}} \text{cis} \frac{(2j-1)\pi}{\rho\alpha_1}, \text{ for } j = 1, 2, 3, \dots, \rho\alpha_1 \quad (23)$$

is obtained by means of the De-Moivre rules such that it is $\text{cis}\pi = \cos\pi + i\sin\pi$ for $i = \sqrt{-1}$. We have

$$|\text{Arg}(\lambda_j)| = \frac{\pi}{\rho\alpha_1}, \frac{3\pi}{\rho\alpha_1}, \dots, \frac{(2\rho\alpha_1-1)\pi}{\rho\alpha_1} \quad (24)$$

If the stability conditions in Lemma 2 are applied; then

$$\frac{\pi}{\rho\alpha_1}, \frac{3\pi}{\rho\alpha_1}, \dots, \frac{(2\rho\alpha_1-1)\pi}{\rho\alpha_1} > \frac{\pi}{2\rho}$$

and so,

$$\frac{1}{\alpha_1}, \frac{3}{\alpha_1}, \dots, \frac{(2\rho\alpha_1-1)}{\alpha_1} > \frac{1}{2}$$

$$\alpha_1 < \min\{2, 6, \dots, 2(2\rho\alpha_1-1)\} \quad (25)$$

are obtained. In the introduction of proposed model in the system (5), it is stated that $\alpha_i \in (0, 1]$ for $i = 1, 2, 3$. Therefore, Eqs. (23) for (20-a) are already satisfied. This means that the stability conditions for the equilibrium point $E(\bar{v}, \bar{n}_1, \bar{n}_2)$ are not disturbed.

Thus, it should be examined whether the equations in (20-b) and (20-c) satisfy the stability conditions. Consider that $\bar{n}_1 = C$ for the equilibrium points both E_1 and E_2 , the equations in (20-b) and (20-c) have the following forms:

$$\lambda^{m\alpha_2} = -r_1 \quad (26)$$

$$\lambda^{m\alpha_3} = r_2 - \frac{2r_2\bar{n}_2}{C}. \quad (27)$$

Since $-r_1 < 0$ due to inequality in (6), it is clear that (26) does not disturb the stability conditions when it is considered similarly to (20). From (27), if

$$\bar{n}_2 > \frac{C}{2}, \quad (28)$$

then the equilibrium point is stable, since $\lambda^{\rho\alpha_3} \in \mathbb{R}^-$. Thus, the following results are achieved.

- (i) Let $\mathcal{R}_0 \leq 1$. It is $\bar{n}_2 = C \frac{1+\sqrt{(1-\mathcal{R}_0)}}{2}$ for E_1 . The LAS conditions in terms of (25) are fulfilled, when $\mathcal{R}_0 < 1$. Therefore, E_1 is LAS.
- (ii) Let $0 < \mathcal{R}_0 \leq 1$. In this case, we have $\bar{n}_2 = C \frac{1-\sqrt{(1-\mathcal{R}_0)}}{2}$ for E_2 . Considering (25), E_2 is unstable point.

The abovementioned results regarding the equilibrium points are submitted in Table 1.

Table 1. LAS conditions of equilibrium points of the system(5).

Equilibrium Point	Existence Condition	Stability Condition
$E_1 \left(\frac{A}{\beta}, C, C \frac{1+\sqrt{(1-\mathcal{R}_0)}}{2} \right)$	If $\mathcal{R}_0 \leq 1$,	If $\mathcal{R}_0 < 1$
$E_2 \left(\frac{A}{\beta}, C, C \frac{1-\sqrt{(1-\mathcal{R}_0)}}{2} \right)$	If $0 < \mathcal{R}_0 \leq 1$,	Unstable point

4. Numerical studies

In this section, the parameters used in the system (5) are given numerical values and this system is analyzed numerically to be compatible with the outcomes of the qualitative analysis. The parameter values are as shown in Table 2.

Table 2. The considered values of parameters in the proposed model (5) and their interpretations.

Parameters	Definitions	Values
A	Applied voltage constant	10.5
β	Decrease rate of voltage constant	1
r_1	Growth rate of core refractive index	0.2
C	Maximum magnitude of the cladding refractive index	15
r_2	Growth rate of cladding refractive index	0.25
δ	The rate of voltage-dependent decrease in cladding refractive index	0.8
n_0	Environmental refractive index	8
$(\alpha_1, \alpha_2, \alpha_3)$	Fractional-orders	(1, 1, 1) (0.9, 0.9, 0.9) (0.75, 0.75, 0.75) (0.7, 0.8, 0.9) (0.9, 0.8, 0.7)
(v_0, n_{10}, n_{20})	Initial conditions	(16, 12, 9)

The following figures show the stability of the equilibrium point E_1 (10.5, 15, 13.17890832929182), since $0 \leq \mathcal{R}_0 = 0.42666667 < 1$.

Table 3. Sensitivity indices of \mathcal{R}_0 according to Table (2).

Parameters	Sensitivity index $(^S)$	in-	Elasticity
r_2	$(^S)\mathcal{R}_{0r_2}^1 = \frac{-4}{Cr_2^2} \left(\delta \frac{A}{\beta} - n_0 \right) = \frac{-1}{r_2} \mathcal{R}_0$	=	-1.7066
δ	$(^S)\mathcal{R}_{0\delta}^1 = \frac{4}{Cr_2} \left(\delta \frac{A}{\beta} - n_0 \right) = \frac{4}{Cr_2} \frac{A}{\beta}$	=	11.2
A	$(^S)\mathcal{R}_{0A}^1 = \frac{4}{Cr_2} \left(\delta \frac{A}{\beta} - n_0 \right) = \frac{4}{Cr_2} \frac{\delta}{\beta}$	=	0.8533
β	$(^S)\mathcal{R}_{0\beta}^1 = \frac{4}{Cr_2} \left(\delta \frac{A}{\beta} - n_0 \right) = \frac{-4}{Cr_2} \delta \frac{A}{\beta^2}$	=	-8.96
C	$(^S)\mathcal{R}_{0C}^1 = \frac{-4}{C^2 r_2} \left(\delta \frac{A}{\beta} - n_0 \right) = \frac{-1}{C} \mathcal{R}_0$	=	-0.0284
n_0	$(^S)\mathcal{R}_{0n_0}^1 = \frac{4}{Cr_2} \left(\delta \frac{A}{\beta} - n_0 \right) = -\frac{4}{Cr_2}$	=	-1.0666

The parameter with the greatest positive effect on \mathcal{R}_0 is δ , while the parameter with the greatest negative effect is β . If δ is increased (or decreased) by 1%, then the value of \mathcal{R}_0 will increase (or decrease) by 10.6667%. Similarly, if β is increased (or decreased) by 1%, then the value of \mathcal{R}_0 will decrease (or increase) by 8%.

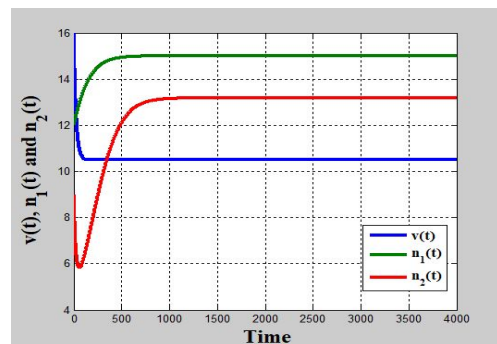


Figure 4. Stabilities of variables for derivative orders given by (1,1,1).

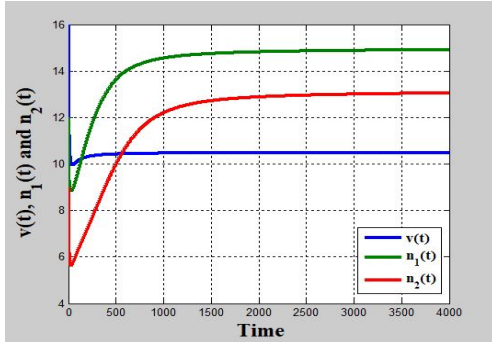


Figure 5. Stabilities of variables for derivative orders given by (.9,.9,.9).

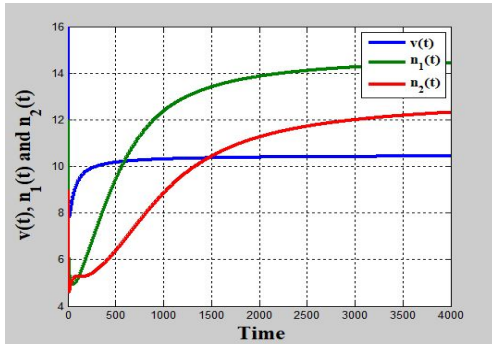


Figure 6. Stabilities of variables for derivative orders given by (.75,.75,.75).

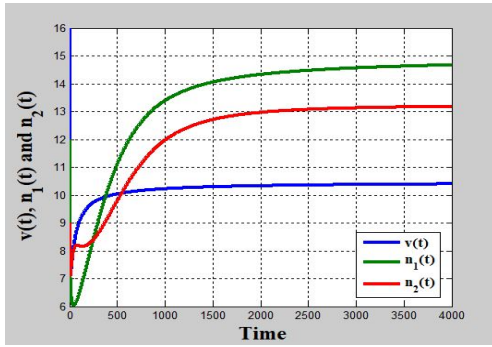


Figure 7. Stabilities of variables for derivative orders given by (.7,.8,.9).

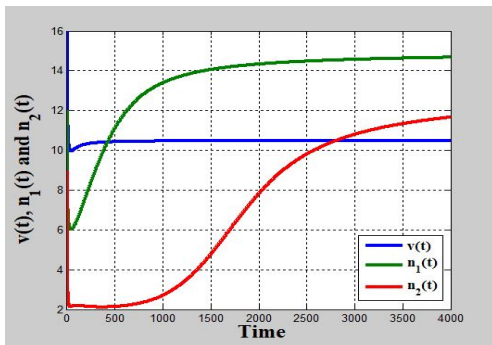


Figure 8. Stabilities of variables for derivative orders given by (.9,.8,.7).

5. Conclusion

In this study, which proposes optical fiber with EO cladding unlike the literature, a mathematical model in the IFOS form in the Caputo meaning including optical fiber variables, given as numerical aperture, critical angle and acceptance angle are presented. The stability analysis consequences of system have been shown with simulations and it has been seen that they are consistent with respect to qualitative analysis.

In the following results as a contribution to the literature, the structural parameters including numerical aperture, critical angle and acceptance angle of optical fiber waveguides are mentioned. In the light of the information given in Table 1, the necessary calculations were made for the stable equilibrium point $E_1 \left(\frac{A}{\beta}, C, C \frac{1+\sqrt{(1-\mathcal{R}_0)}}{2} \right)$ at $\mathcal{R}_0 < 1$.

Result 1 Since the critical angle formula is $\theta_c = \arcsin \left(\frac{n_2}{n_1} \right)$, this value evaluated at the LAS E_1 is obtained as

$$\bar{\theta}_c = \arcsin \left(\frac{1+\sqrt{(1-\mathcal{R}_0)}}{2} \right) \text{ for } 0 \leq \mathcal{R}_0 < 1, \quad (29)$$

such that $-\frac{\pi}{2} \leq \bar{\theta}_c \leq \frac{\pi}{2}$.

Result 2 Let us consider that the numerical aperture formula given as $NA = n_0 \sin \theta_a = \sqrt{n_1^2 - n_2^2}$. When E_1 is LAS, this formula is

$$NA = \frac{C}{2} \sqrt{2 + \mathcal{R}_0 - 2\sqrt{(1-\mathcal{R}_0)}} \text{ for } 0 \leq \mathcal{R}_0 < 1. \quad (30)$$

Result 3 Acceptance angle for the LAS E_1 is obtained as

$$\bar{\theta}_a = \arcsin \left(\frac{C}{2n_0} \sqrt{2 + \mathcal{R}_0 - 2\sqrt{(1-\mathcal{R}_0)}} \right) \text{ for } 0 \leq \mathcal{R}_0 < 1. \quad (31)$$

such that $-\frac{\pi}{2} \leq \bar{\theta}_a \leq \frac{\pi}{2}$.

Consider the point E_1 for $\mathcal{R}_0 < 1$, the results obtained above are summarized in the table below.

Table 4. The obtained results of the proposed system in (5) for $0 \leq \mathcal{R}_0 < 1$.

The LAS equilibrium point	$E_1 \left(\frac{A}{\beta}, C, C \frac{1+\sqrt{(1-\mathcal{R}_0)}}{2} \right)$
The critical angle formula for E_1	$\bar{\theta}_c = \arcsin \left(\frac{1+\sqrt{(1-\mathcal{R}_0)}}{2} \right)$
The numerical aperture formula for E_1	$\overline{NA} = \frac{C}{2} \sqrt{2 + \mathcal{R}_0 - 2\sqrt{(1 - \mathcal{R}_0)}}$
The acceptance angle formula for E_1	$\bar{\theta}_a = \arcsin \left(\frac{C}{2n_0} \sqrt{2 + \mathcal{R}_0 - 2\sqrt{(1 - \mathcal{R}_0)}}$

Considering the values in Table 2, the values in Table 3 are obtained as follows:

- Threshold parameter: $0 \leq \mathcal{R}_0 = 0.42666667 < 1$,
- The LAS equilibrium point: $E_1(10.5, 15, 13.1789)$,
- The critical angle: $\bar{\theta}_c = \arcsin(0.8785) = 61.46194534^\circ$,
- The numerical aperture formula: $\overline{NA} = 7.163544880024326$,
- The acceptance angle: $\bar{\theta}_a = \arcsin(0.8954) = 63.55985484^\circ$.

As a result, considering these assumptions, the fiber optic cable, the numerical aperture, the critical angle, and the acceptance angle values can be accordingly recalculated by the obtained formulas. In addition, the above-mentioned structural parameter values can be easily found according to the parameter values of the system.

In the scope of our study, we introduced an innovative approach by proposing the utilization of an electro-optic material, previously unconsidered, for the protective sheath of the fiber optic

cable. Subsequently, we mathematically modeled the phenomena associated with light behavior. As a result of this analysis, we put forth the proposition that, instead of employing a general formula, calculations for these parameters could be conducted using the novel equations derived from our mathematical modeling.


In the future, such works will be able to guide the mathematical modeling of fibers designed with materials with the proposed adjustable cladding index and will be able to shed light on material development in line with this modeling. The types of materials to be developed in this way can be the subject of research in many fields, especially in materials engineering. The results obtained can be revolutionary in many fields.

References


- [1] Addanki, S., Amiri, I. S., & Yupapin, P. (2018). Review of optical fibers-introduction and applications in fiber lasers. *Results in Physics*, 10, 743-750.
- [2] Sharma, P., Pardeshi, S., Arora, R.K. & Singh, M. (2013). A Review of the Development in the Field of Fiber Optic Communication Systems. *International Journal of Emerging Technology and Advanced Engineering*, 3(5), 2250-2459.
- [3] Chu, P.L. (2009). *Fiber Optic Devices and Systems. Electrical Engineering - Volume II 113*. EOLSS Publications.
- [4] Born, M., Wolf, E. (1999). *Principles of Optics: Electromagnetic Theory of Propagation, Interference and Diffraction of Light*. 6th ed. Cambridge University Press.
- [5] Shirley, J.W. (2005). An Early Experimental Determination of Snell's Law. *American Journal of Physics*, 19(9), 507.
- [6] Bryant, F. (1958). Snell's Law of Refraction. *Physics Bulletin*, 9(12), 317.
- [7] Martín-Fernandez, M.L., Tynan, C.J., & Webb, S.E.D. (2013). A 'pocket guide' to total internal reflection fluorescence. *Journal of Microscopy*, 252(1), 16-22.
- [8] Senior, J. M. (2009). *Optical Fiber Communications Principles and Practice Third Edition*. Kirby Street, London
- [9] Axelrod, D., Burghardt, T. P. & Thompson, N. L. (1984) Total internal reflection fluorescence. *Annual Review of Biophysics and Bioengineering*, 13(1),247-268.
- [10] Wadsworth, W.J., Percival, R.M., Bouwmans, G., Knight, J.C., Birks, T.A., Hedley, T.D., & Russell, P. St J. (2004). Very High Numerical Aperture Fibers. *IEEE Photonics Technology Letters*, 16(3), 843-845.
- [11] Dragic, P.D., Cavillon, M., & Ballato, J. (2018). Materials for optical fiber lasers: A review. *Applied Physics Reviews*, 5(4), 041301.
- [12] Kao, K. C. & Hockham, G.A.(1997). Dielectric-fibre surface waveguides for optical frequencies. *Elektron*, 14(5), 11-12.
- [13] Peng, G.D., Ji, P., & Chu, P.L. (2002). Electro-optic polymer optical fibers and their device applications. *SPIE*, 4459, 101-117.

- [14] Welker, D.J., Garvey, D.W., Breckon, C. D., & Kuzyk, M.G. (1999). Single-mode Electrooptic Polymer Optical Fiber. *Organic Thin Films for Photonic Applications*, SaC1.
- [15] Welker, D.J., Tostenrude, J., Garvey, D.W., Canfield, B.K. & Kuzyk, M.G. (1998). Fabrication and characterization of single-mode electro-optic polymer optical fiber. *Optics Letters*, 23(23), 1826.
- [16] Singer, K. D., Kuzyk, M. G., Holland, W. R., Sohn, J.E., Lalama, S.J., Comizzoli, R.B., Katz, H.E., & Schilling, M. L. (1998). Electro-optic phase modulation and optical second-harmonic generation in corona-poled polymer films. *Applied Physics Letters*, 53(19), 1800.
- [17] Canfield, B.K., Kuzyk, M.G., & Welker, D.J. (1999). Nonlinear characterization of polymer electro-optic fiber. In *Organic Nonlinear Optical Materials*, 3796, 313-319. <https://doi.org/10.1117/12.368289>.
- [18] Kuzyk, M.G., Garvey, D.W., Canfield, B.K., Vigil, S.R., Welker, D.J., Tostenrude, J., & Breckon, C. (1999). Characterization of single-mode polymer optical fiber and electrooptic fiber devices. *Chemical Physics*, 245(1-3), 327-340.
- [19] Garvey, D.W. & Kuzyk, M.G. (1999). Nonlinear optics in polymer optical fibers. (1999). In *Organic Nonlinear Optical Materials*, <https://doi.org/10.1117/12.368283>, 3796, 13-20.
- [20] Ali, Z., Rabiei, F., Rashidi, M.M., & Khodadadi, T. (2022). A fractional-order mathematical model for COVID-19 outbreak with the effect of symptomatic and asymptomatic transmissions. *The European Physical Journal Plus*, 137(3), 1-20.
- [21] Delavari, H., Baleanu, D., & Sadati, J. (2012). Stability analysis of Caputo fractional-order nonlinear systems revisited. *Nonlinear Dynamics*, 67(4), 2433-2439.
- [22] Du, M., Wang, Z. & Hu, H. (2013). Measuring memory with the order of fractional derivative. *Scientific Reports*, 3(1), 1-3.
- [23] Xie, L., Shi, J., Yao, J., & Wan, D. (2022). Research on the Period-Doubling Bifurcation of Fractional-Order DCM Buck-Boost Converter Based on Predictor-Corrector Algorithm. *Mathematics*, 10(12), 1993.
- [24] Baleanu, B., Guvenc, Z.B., & Machado, J.A.T. (2010). New Trends in Nanotechnology and Fractional Calculus Applications. *New Trends in Nanotechnology and Fractional Calculus Applications*, 10, 978-90, New York: Springer.
- [25] Abro, K.A. (2021). Role of fractal-fractional derivative on ferromagnetic fluid via fractal Laplace transform: A first problem via fractal-fractional differential operator. *European Journal of Mechanics - B/Fluids*, 85, 76-81.
- [26] Abro, K.A. & Atangana, A. (2020). Mathematical analysis of memristor through fractal-fractional differential operators: A numerical study. *Mathematical Methods in the Applied Sciences*, 43(10), 6378-6395.
- [27] Podlubny, I. (1999). *Fractional differential equations: an introduction to fractional derivatives, fractional differential equations, to methods of their solution and some of their applications*. Academic Press, San Diego
- [28] Odibat, Z.M., Shawagfeh, N.T. (2007). Generalized Taylor's formula. *Applied Mathematics and Computation*, 186(1), 286-293.
- [29] Daşbaşı, B. (2023). Fractional order bacterial infection model with effects of anti-virulence drug and antibiotic. *Chaos, Solitons & Fractals*, 170, 113331.
- [30] Deng, W., Li, C., & Guo, Q. (2007). Analysis of fractional differential equations with multi-orders. *Fractals*, 15(2), 173-182.
- [31] Tavazoei, M., Asemani, M.H. (2020). Robust stability analysis of incommensurate fractional-order systems with time-varying interval uncertainties. *Journal of the Franklin Institute*, 357(18), 13800-13815.
- [32] Daşbaşı, B. (2020). Stability analysis of the hiv model through incommensurate fractional-order nonlinear system. *Chaos, Solitons & Fractals*, 137(109870),
- [33] Daşbaşı, B., & Daşbaşı, T. (2017). Mathematical analysis of Lengyel-Epstein chemical reaction model by fractional-order differential equation's system with multi-orders. *International Journal of Science and Engineering Investigations*, 6(70), 78-83.
- [34] Li, H. L., Zhang, L., Hu, C., Jiang, Y. L., & Teng, Z. (2017). Dynamical analysis of a fractional-order predator-prey model incorporating a prey refuge. *Journal of Applied Mathematics and Computing*, 54, 435-449.

Büşra Ersoy was born on March 8, 1997, in Kayseri. She took English preparatory education for one year in the 2015-2016 academic year. Then she received a BS degree from the Electrical and Electronics Engineering Department of Erciyes University, Kayseri in 2020. In 2021, she started her Master's Education in the Electronics Engineering Department at Kayseri University. She is currently working as a researcher assistant in the research project titled "Design, Fabrication, and Characterization of Meta-Lenses for Infrared and Visible Wavelengths" and has a Graduate Research Scholarship supported by the Scientific and Technological Research Council of Turkey (TUBİTAK-ARDEB-121E518).

 <https://orcid.org/0000-0003-1383-3311>


Bahatdin Daşbaşı received a BS degree in Mathematics from Ankara University in 2002, the MS degree in the field of applied statistic in Mathematics department from the Niğde University in 2005 and a Ph.D. degree in the field of applied mathematics in mathematics department from the Erciyes University in 2016. He also has the title of Associate Professor in Mathematics since 2021. He is still working as an associate professor at the Department of Basic Engineering Sciences, Faculty of Engineering, Architecture and Design, Kayseri University. His current research interests include fractional order differential equations, mathematical modeling, stability analysis, and artificial neural networks.

 <https://orcid.org/0000-0001-8201-7495>

Ekin Aslan received the BS degree in 2004 from the Electronics Engineering Department of Erciyes University, MS degree in 2011 from the Electrical and Electronics Engineering of Mustafa Kemal University,

and PhD degree in 2017 from the Electrical and Electronics Engineering Department of Erciyes University. Dr. Aslan was a recipient of the Doctoral Research Fellowship from the Scientific and Technological Research Council of Turkey (TUBITAK) (2214-A). She worked as an Assistant Professor in the Departments of Electrical and Electronics Engineering at

Nuh Naci Yazgan University and Hatay Mustafa Kemal University. She is currently working as an Associate Professor in the Electrical and Electronics Engineering Department of Kayseri University. Her research interests include integrated plasmonic systems for bio-detection, vibrational spectroscopy, plasmonic metamaterials, computational and experimental electromagnetics, and nanophotonic devices.

 <https://orcid.org/0000-0003-0933-7796>

Appendix A

Matlab codes used for graphics are:

memory.m

```

1
2 function [yo] = memory(r, c, k)
3 temp = 0;
4 for j=1:k-1
5 temp = temp + c(j)*r(k-j);
6 end
7 yo = temp;

```

fiber_optic_function.m

```

1 function [T, Y] = fiber\_optic\_function(parameters, orders, TSim, Y0)
2 h = .04;
3 n = round(TSim/h);
4 q1 = orders(1); q2 = orders(2); q3 = orders(3);
5 a\_1 = parameters(1); b = parameters(2); r\_1 = parameters(3);
6 C = parameters(4); r\_2 = parameters(5); a\_2 = parameters(6);
7 n\_3 = parameters(7);
8 cp1 = 1; cp2 = 1; cp3 = 1;
9 for j = 1:n
10 c1(j) = (1-(1+q1)/j)*cp1;
11 c2(j) = (1-(1+q2)/j)*cp2;
12 c3(j) = (1-(1+q3)/j)*cp3;
13 cp1 = c1(j); cp2 = c2(j); cp3 = c3(j);
14 end
15
16 x(1) = Y0(1); y(1) = Y0(2); z(1) = Y0(3);
17
18 for i = 2:n
19 x(i) = (a\_1-b*x(i-1))*h*\mathrm{\wedge}$q1 - memory(x, c1, i);
20 y(i) = (r\_1*y(i-1)*(1-y(i-1)/C))*h*\mathrm{\wedge}$q2 -memory(y, c2,
    i);
21 z(i) = (r\_2*z(i-1)*(1-z(i-1)/y(i-1))-a\_2*x(i-1)+n\_3)*h*\mathrm{\
    wedge}$q3 - memory(z, c3, i);
22 end
23
24 for j = 1:n
25 Y(j,1) = x(j); Y(j,2) = y(j); Y(j,3) = z(j);
26 end
27
28 T = 0:h:TSim;

```

run.m

```

1 close all; clear all; clc;
2 A = 1:4000;
3 A = A';

```

```

4 [t, y] = fiber\_optic\_function ([10.5 1 .2 15 .25 .8 8], [1 1 1],
   160, [16 12 9]);
5 figure; plot(A,y(:,1), A,y(:,2),A,y(:,3));
6 xlabel('\textbackslashbf Time', 'fontsize', 10); ylabel('\
   \textbackslashbf v(t), n\_1(t) and n\_2(t)', 'fontsize', 10); grid;
7 legend('v(t)', 'n\_1(t)', 'n\_2(t)');
8 title('Stabilities of variables for derivative orders given by (1,1,1)
   ');
9
10 [t, y] = fiber\_optic\_function ([10.5 1 .2 15 .25 .8 8], [.9 .9 .9],
   160, [16 12 9]);
11 figure; plot(A,y(:,1), A,y(:,2),A,y(:,3));
12 xlabel('\textbackslashbf Time', 'fontsize', 10); ylabel('\
   \textbackslashbf v(t), n\_1(t) and n\_2(t)', 'fontsize', 10); grid;
13 legend('v(t)', 'n\_1(t)', 'n\_2(t)');
14 title('Stabilities of variables for derivative orders given by
   (.9,.9,.9)');
15
16 [t, y] = fiber\_optic\_function ([10.5 1 .2 15 .25 .8 8], [.75 .75
   .75], 160, [16 12 9]);
17 figure; plot(A,y(:,1), A,y(:,2),A,y(:,3));
18 xlabel('\textbackslashbf Time', 'fontsize', 10); ylabel('\
   \textbackslashbf v(t), n\_1(t) and n\_2(t)', 'fontsize', 10); grid;
19 legend('v(t)', 'n\_1(t)', 'n\_2(t)');
20 title('Stabilities of variables for derivative orders given by
   (.75,.75,.75)');
21
22 [t, y] = fiber\_optic\_function ([10.5 1 .2 15 .25 .8 8], [.7 .8 .9],
   160, [16 12 9]);
23 figure; plot(A,y(:,1), A,y(:,2),A,y(:,3));
24 xlabel('\textbackslashbf Time', 'fontsize', 10); ylabel('\
   \textbackslashbf v(t), n\_1(t) and n\_2(t)', 'fontsize', 10); grid;
25 legend('v(t)', 'n\_1(t)', 'n\_2(t)');
26 title('Stabilities of variables for derivative orders given by
   (.7,.8,.9)');
27
28 [t, y] = fiber\_optic\_function ([10.5 1 .2 15 .25 .8 8], [.9 .8 .7],
   160, [16 12 9]);
29 figure; plot(A,y(:,1), A,y(:,2),A,y(:,3));
30 xlabel('\textbackslashbf Time', 'fontsize', 10); ylabel('\
   \textbackslashbf v(t), n\_1(t) and n\_2(t)', 'fontsize', 10); grid;
31 legend('v(t)', 'n\_1(t)', 'n\_2(t)');
32 title('Stabilities of variables for derivative orders given by
   (.9,.8,.7)');

```

